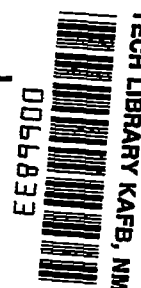


10547

NACA TN 4208



NATIONAL ADVISORY COMMITTEE FOR AERONAUTICS

TECHNICAL NOTE 4208

TURBULENT BOUNDARY LAYER ON A YAWED CONE
IN A SUPERSONIC STREAM

By Willis H. Braun

Lewis Flight Propulsion Laboratory
Cleveland, Ohio



Washington

January 1958

ATMDC
TECHNICAL LIBRARY
APR 23 1958



0066833

NATIONAL ADVISORY COMMITTEE FOR AERONAUTICS

TECHNICAL NOTE 4208

TURBULENT BOUNDARY LAYER ON A YAWED CONE IN A SUPERSONIC STREAM

By Willis H. Braun

SUMMARY

The momentum integral equations are derived for the boundary layer on an arbitrary curved surface, using a streamline coordinate system. Computations of the turbulent boundary layer on a slightly yawed cone are made for a Prandtl number 0.70, wall to free-stream temperature ratios of $1/2$, 1, and 2, and Mach numbers from 1 to 4. Deflection of the fluid in the boundary layer from outer stream direction, local friction coefficient, displacement surface, lift coefficient, and pitching-moment coefficient are presented.

INTRODUCTION

The flow of a laminar boundary layer over a cone in a supersonic stream has been well established, not only when the cone is aligned with the free stream (refs. 1 and 2) but also for certain perturbed motions. Moore (refs. 3 and 4) has computed the boundary layer on a cone at angle of attack, and Illingworth (ref. 5) has found the flow when the cone is spinning. Recently, the laminar boundary layer for a cone that is both spinning and at angle of attack has been investigated (refs. 6 and 7).

The corresponding treatment of the turbulent boundary layer on a cone has only been begun. Van Driest (ref. 8) and Gazley (ref. 9) have studied the cone at zero angle of attack. They have found transformations relating boundary layers on cones to those on flat plates. Van Driest's method represents the turbulent stresses according to the mixing-length theory, while Gazley uses the momentum-integral equations.

The investigation of the cone at yaw (attack) or in spin is impeded by the lack of any generalization of the turbulent stress representations to three-dimensional boundary layers. Moreover, it appears from experimental measurement (see ref. 10 for review of experimental results) that the "principle of independence" may not hold for three-dimensional turbulent boundary layers. That is, on a yawed cylindrical surface, the flow in the plane normal to the axis may not develop independently of that along the generators, as in laminar, incompressible flow. From

4372

CP-1

these considerations it appears that a resolution of the equations of motion along a body coordinate system will not, in general, lead to a tractable problem. More appropriate for this case is the integral method as applied by Mager (ref. 11), which follows the development of the boundary layer along a streamline, assuming that the thickness, skin friction, and other properties behave nearly as in plane flow.

The following development extends Mager's use of the integral method to compressible flow over arbitrary curved surfaces. The specific case of the turbulent boundary layer on a cone at small angle of yaw is considered. The forces exerted by the boundary layer on the cone and the heat transfer to the surface are computed.

SYMBOLS

A	defined in equation (19)
B	defined in equation (18)
C	constant
C_D	frictional drag coefficient
C_F	local friction coefficient (defined in eq. (12))
C_L	frictional lift coefficient
C_M	pitching-moment coefficient
D	defined in equation (51)
F	defined in equation (42)
F_D	frictional drag force
F_L	frictional lift force
g	determinant of metric coefficients
g_{ij}	metric coefficients
I	integral
K	constant
$L_0, L_1, N_1, P_1, R_0, R_1$	defined in equation (40)

4372

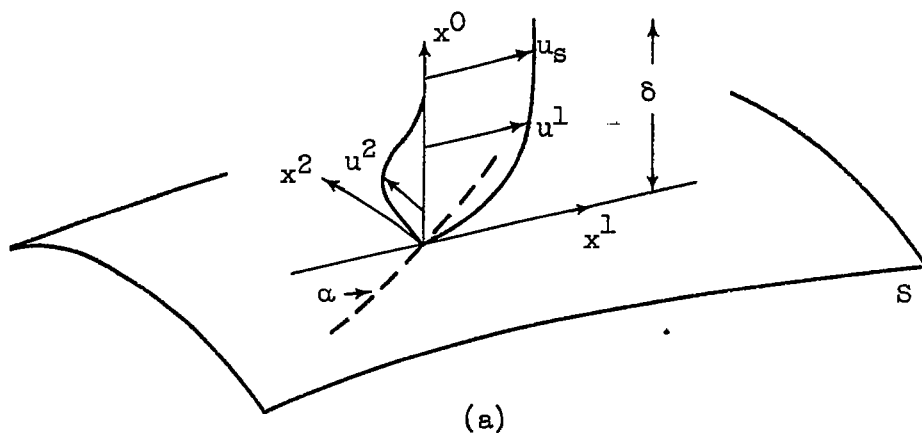
\bar{M}	Mach number on surface of unyawed cone
M_s	Mach number on surface of yawed cone
M_1	Mach number ahead of shock
M	pitching moment
n	index, equation (15)
Pr	Prandtl number
p	pressure
r	distance from apex of cone
St	Stanton number
$s(i)$	arc length in i^{th} direction
T	temperature
t	time
u	velocity component in direction of cone ray
$u^i, u(i)$	velocity component in i^{th} direction
w	circumferential velocity component
x, z	constants defining potential flow
x^i	coordinate in streamline system of coordinates
α	deflection angle at wall
α_1, α_2	defined in equation (45)
γ	ratio of specific heats
Δ	displacement surface height
δ	boundary-layer thickness
δ_1^*, δ_2^*	displacement thicknesses, equation (11)
ϵ	yaw angle

4372

CP-1 back

η	parameter defining pressure in potential flow
Θ	cone half-angle
$\theta_{11}, \theta_{21}, \theta_{22}$	momentum thicknesses, equation (11)
λ	yaw parameter
μ	viscosity
ν	kinematic viscosity
ξ	parameter defining density in potential flow
ρ	density
τ_j^i, τ_{ij}	viscous stress
ϕ	angle about wind axis
ψ	angle about body axis
Subscripts:	
m	mean value
s	stream value
w	wall value
Superscript:	
—	value on unyawed cone

INTEGRAL EQUATIONS ON A CURVED SURFACE



Consider the boundary layer of thickness δ on the surface S of sketch (a). The projection of the stream velocity u_s on the surface determines the x^1 direction. (It is assumed that u_s is the velocity a potential flow would have at the surface.) The direction in the plane of the surface normal to x^1 is designated x^2 . With the choice of x^0 normal to the surface the result is a right-handed orthogonal system. There can, in general, be a pressure gradient in the x^2 direction. The effect of the pressure gradient is much stronger upon the low-energy fluid in the boundary layer than upon the outer stream. Consequently, u^2 does not vanish in the boundary layer, and the turning of the streamlines within the boundary layer is greater than at $x^0 = \delta$. The angle of deflection between the outer streamline and the limiting direction of the streamlines at the surface is denoted by α .

The element of arc ds in the x -system is given by

$$(ds)^2 = g_{00}(dx^0)^2 + g_{11}(dx^1)^2 + g_{22}(dx^2)^2$$

where the g_{ii} are the metric coefficients. Of these, g_{11} and g_{22} are functions of x^0, x^1, x^2 determined by the surface S . By choosing x^0 to be the normal distance from S , it is correct to set $g_{00} \equiv 1$. With the definition

$$g \equiv |g_{ij}| = g_{11}g_{22}$$

the equation of continuity becomes (ref. 12)

$$\sum_{i=0}^2 \left[\frac{\partial}{\partial x^i} (\rho u^i) + \frac{1}{2} \rho u^i \frac{\partial}{\partial x^i} \ln g \right] = 0 \quad (1)$$

The momentum equations are (as derived from ref. 12)

$$\sum_{l=0}^2 \left(\rho u^l u^i_{,l} + \frac{1}{g_{11}} \frac{\partial p}{\partial x^1} - \frac{1}{g_{22}} \tau^i_{2,2} \right) = 0 \quad i = 0, 1, 2 \quad (2)$$

In equation (2) $u^i_{,l}$ is the covariant derivative of the contravariant vector u^i with respect to x^l , and τ^i_l is the stress tensor excluding pressure.

It is more convenient later to have (1) and (2) in terms of the physical components of the velocities and stresses. The physical components are given by

$$u(i) = \sqrt{g_{ii}} u^i \quad (3)$$

$$\tau(ij) = \sqrt{\frac{g_{ii}}{g_{jj}}} \tau_j^i \quad (4)$$

and the arc lengths in the three coordinate directions are

$$ds(i) = \sqrt{g_{ii}} dx^i \quad (5)$$

If, in addition, the results of the appendix are used to choose the dominant turbulent force terms, equations (1) and (2) become, respectively,

$$\sum_{i=0}^2 \left[\frac{\partial \rho u(i)}{\partial s(i)} + \rho u(i) \frac{\partial}{\partial s(i)} \ln \sqrt{\frac{g}{g_{ii}}} \right] = 0 \quad (6)$$

and

$$\begin{aligned} \sum_{i=0}^2 \left[\rho u(i) \frac{\partial u(1)}{\partial s(i)} \right] + \rho u(0) u(1) \frac{\partial \ln \sqrt{g_{11}}}{\partial s(0)} + \rho u(1) u(2) \frac{\partial \ln \sqrt{g_{11}}}{\partial s(2)} \\ - \rho u^2(2) \frac{\partial}{\partial s(1)} \ln \sqrt{g_{22}} = \frac{\partial \tau(01)}{\partial s(0)} - \frac{\partial p}{\partial s(1)} \end{aligned} \quad (7)$$

$$\begin{aligned} \sum_{i=0}^2 \left[\rho u(i) \frac{\partial u(2)}{\partial s(i)} \right] + \rho u(0) u(2) \frac{\partial \ln \sqrt{g_{22}}}{\partial s(0)} + \rho u(1) u(2) \frac{\partial \ln \sqrt{g_{22}}}{\partial s(1)} \\ - \rho u^2(1) \frac{\partial \ln \sqrt{g_{11}}}{\partial s(2)} = \frac{\partial \tau(02)}{\partial s(0)} - \frac{\partial p}{\partial s(2)} \end{aligned} \quad (8)$$

Outside the boundary layer, equations (7) and (8) become

$$\rho_s u_s \frac{\partial u_s}{\partial s(1)} = - \frac{\partial p}{\partial s(1)} \quad (9)$$

and

$$\rho_s u_s^2 \frac{\partial \ln \sqrt{g_{11}}}{\partial s(2)} = \frac{\partial p}{\partial s(2)} \quad (10)$$

Equations (7) and (8) are now to be integrated across the boundary layer making use of (6), (9), (10), and the following definitions of displacement and momentum thicknesses:

$$\left. \begin{aligned} \delta_1^* &= \int_0^\delta \left[1 - \frac{\rho u(1)}{\rho_s u_s} \right] dx^0 \\ \theta_{11} &= \int_0^\delta \left[1 - \frac{u(1)}{u_s} \right] \frac{\rho u(1)}{\rho_s u_s} dx^0 \\ \delta_2^* &= - \int_0^\delta \frac{\rho u(2)}{\rho_s u_s} dx^0 \\ \theta_{21} &= - \int_0^\delta \frac{u(2)}{u_s} \frac{\rho u(1)}{\rho_s u_s} dx^0 \\ \theta_{22} &= - \int_0^\delta \frac{u(2)}{u_s} \frac{\rho u(2)}{\rho_s u_s} dx^0 \end{aligned} \right\} \quad (11)$$

The result is

$$\begin{aligned} \frac{\partial \theta_{11}}{\partial s(1)} + \theta_{11} \frac{\partial}{\partial s(1)} \ln \rho_s u_s^2 \sqrt{g_{22}} + \delta_1^* \frac{\partial}{\partial s(1)} \ln u_s + \frac{\partial \theta_{21}}{\partial s(2)} \\ + \theta_{21} \frac{\partial}{\partial s(2)} \ln \rho_s u_s^2 g_{11} - \theta_{22} \frac{\partial}{\partial s(1)} \ln \sqrt{g_{22}} - \frac{\partial \delta_2^*}{\partial s(2)} \\ - \delta_2^* \frac{\partial}{\partial s(2)} \ln \rho_s u_s \sqrt{g_{11}} = \frac{\tau(01)_w}{\rho_s u_s^2} \equiv \frac{1}{2} C_f \end{aligned} \quad (12)$$

$$\begin{aligned} \frac{\partial \theta_{21}}{\partial s(1)} + \theta_{21} \frac{\partial}{\partial s(1)} \ln \rho_s u_s^2 g_{22} + \frac{\partial \theta_{22}}{\partial s(2)} + \theta_{22} \frac{\partial}{\partial s(2)} \ln \rho_s u_s^2 \sqrt{g_{11}} \\ - (\theta_{11} + \delta_1^*) \frac{\partial}{\partial s(2)} \ln \sqrt{g_{11}} = \frac{1}{2} C_f \frac{\tau(02)_w}{\tau(01)_w} = \frac{1}{2} C_f \tan \alpha \end{aligned} \quad (13)$$

In deriving (12) and (13) use has been made of the fact that the metric coefficients change very little over the thickness δ of the boundary

layer, so that (ref. 12)

$$\left. \begin{aligned} \frac{\partial}{\partial s(1)} \ln \sqrt{g_{1j}} &= \frac{\partial}{\partial s(1)} \ln \sqrt{g_{1j}} \Big|_{x^0=0} \left[1 + \mathcal{O}\left(\frac{\delta}{R}\right) \right] \\ \frac{\partial}{\partial s(2)} \ln \sqrt{g_{1j}} &= \frac{\partial}{\partial s(2)} \ln \sqrt{g_{1j}} \Big|_{x^0=0} \left[1 + \mathcal{O}\left(\frac{\delta}{R}\right) \right] \\ \frac{\partial}{\partial x^0} \ln \sqrt{g} &\sim \frac{1}{R} \end{aligned} \right\} \quad (14)$$

where in each of equations (14) R is some radius of curvature. Terms of order δ/R compared with unity have been neglected in (13).

Equations (12) and (13) govern the development of a compressible boundary layer on a curved surface on those portions of the surface where the radius of curvature is very much greater than the boundary-layer thickness. In this respect the foregoing derivation resembles that of Timman (ref. 13) for laminar, incompressible boundary layers in contrast to that of Mager (ref. 14) for incompressible boundary layers over axisymmetric bodies at yaw.

VELOCITY PROFILES AND FRICTION COEFFICIENT

The five boundary-layer thicknesses (11) that arise in the equations of motion (12) and (13) are functions of the two velocity profiles in the boundary layer $u(1)/u_s$ and $u(2)/u_s$, and of the density ratio ρ/ρ_s . These three unknown variables along with the friction coefficient C_f and the deflection angle α give a total of five. Therefore, hypotheses about the boundary-layer characteristics must be added to the two equations of motion for the system to be solvable. The only hypotheses available are those suggested by studies of the boundary layers on flat surfaces where the streamwise pressure gradient is negligible. It is convenient to write these hypotheses here and to discuss in a subsequent section whether they are appropriate to a cone at yaw.

With respect to the velocity profile in the direction of the free stream, the customary assumption of a power law is made; as in planar flow,

$$\frac{u(1)}{u_s} = \left(\frac{x^0}{\delta} \right)^{1/n} \quad (15)$$

The index n is known to vary roughly as the logarithm of the Reynolds number (ref. 15), although to simplify computations it is usually kept at a constant value of 7 to 9.

The component of crossflow in the boundary layer $u(2)/u_s$ must vanish both at the wall and at the edge of the boundary layer, as shown in sketch (a). An expression which yields a qualitatively correct profile and which is also quantitatively accurate for slow flows (ref. 11) is

$$\frac{u(2)}{u_s} = \left(\frac{x^0}{\delta}\right)^{1/n} \left(1 - \frac{x^0}{\delta}\right)^2 \tan \alpha \quad (16)$$

For the density ratio ρ/ρ_s there is available under the condition of negligible pressure gradient the quadratic in the velocity profile that holds in plane flows (e.g., ref. 8):

$$\frac{\rho}{\rho_s} = \frac{T_s}{T_w} \left[1 + B \frac{u(1)}{u_s} - A^2 \left(\frac{u(1)}{u_s} \right)^2 \right]^{-1} \quad (17)$$

where

$$B \equiv \left(1 + \text{Pr}^{1/3} \frac{\gamma - 1}{2} M_s^2\right) \frac{T_s}{T_w} - 1 \quad (18)$$

$$A^2 \equiv \text{Pr}^{1/3} \frac{\gamma - 1}{2} M_s^2 \frac{T_s}{T_w} \quad (19)$$

The subscript s refers to conditions outside the boundary layer, and T_w is the (constant) temperature of the wall. The factor $\text{Pr}^{1/3}$ is an empirical correction (ref. 16).

Again, using a property of planar flow, the friction coefficient is replaced by a generalized Blasius formula

$$C_f = K \left(\frac{\mu_m}{\mu_s} \right)^{1/4} \left(\frac{T_s}{T_m} \right)^{3/4} \left(\frac{v_s}{u_s \delta} \right)^{1/4} \quad (20)$$

The subscript m refers to reference conditions in the boundary layer. Eckert (ref. 17) gives for a reference temperature

$$T_m = \frac{1}{2} (T_w + T_s) + 0.22 \text{Pr}^{1/3} \frac{\gamma - 1}{2} M_s^2 T_s \quad (21)$$

The value of K is generally taken as about 0.045 for a flat plate and $\frac{2}{\sqrt{3}}$ (0.045) for a cone aligned with the stream.

The relations (15) through (21) reduce the number of dependent variables to two, the thickness δ and the deflection angle α . Stream Mach number and ratio of wall to stream temperature are the parameters. Further progress in the solution of the equations of motion (12) and (13) requires knowledge of the stream of a given configuration (i.e., M_s).

STREAM COORDINATE SYSTEM ON A SLIGHTLY YAWED CONE

The coordinate system on the yawed cone is composed of the potential-flow streamlines on the surface and their orthogonal trajectories. A comparison is made in figure 1 of the flows on the surface of an unwyawed cone and a yawed cone. Whereas the surface streamlines coincide with the elements of an unwyawed cone, on a yawed cone they are deflected by the circumferential pressure gradient.

The potential flow may be found for small yaw angles ϵ by use of the tables of reference 18. (The definition of ϵ used here and in ref. 18 is the negative of that of some treatments.)

In terms of the angle ϕ about the wind axis, and to first order in ϵ , the radial and circumferential components of velocity are given by

$$u = \bar{u} + \epsilon x \cos \phi \quad (22)$$

$$w = \epsilon z \sin \phi \quad (23)$$

where x, z, \bar{u} are coefficients tabulated in reference 18 against cone angle and Mach number. The velocity \bar{u} is recognized as the radial velocity at no yaw ($\epsilon = 0$). When making computations it is necessary (ref. 3) to replace the values of z appearing in reference 18 by $z = -z$ (tables) $-2x/\sin \Theta$. At the surface of the cone it is allowable to first order in ϵ to replace the angle ϕ by the cone angle ψ (ref. 19). Then the path of the streamlines on the surface of the cone is given by

$$\frac{u}{w} = \frac{\frac{dr}{dt}}{r \sin \Theta \frac{d\psi}{dt}} \quad (24)$$

Integration of (24) yields

$$f(x^2) = \frac{1 - \cos \psi}{1 + \cos \psi} \left[r^{\frac{z}{\bar{u}}} (\sin \psi)^{-\frac{x}{\bar{u}} \sin \Theta} \right]^{-2 \frac{\epsilon}{\sin \Theta}} \quad (25)$$

where each value of the parameter x^2 is associated with a streamline. The exponent $\epsilon/\sin \Theta$ appearing in (25) is the parameter describing the perturbation of the system from zero yaw, and is hereinafter denoted as λ :

$$\lambda \equiv \frac{\epsilon}{\sin \Theta} \quad (26)$$

Let the function $f(x^2)$ be chosen so that at zero yaw ($\lambda = 0$) $x^2 = -\cos \psi$. Then

$$f(x^2) = \frac{1 + x^2}{1 - x^2} \quad (27)$$

Equations (25) and (27) taken together are an implicit transformation from r, ψ to x^2 . Their combination yields

$$x^2 = -\cos \psi - \sin^2 \psi \ln r^{z/u} (\sin \psi)^{-(x/u) \sin \Theta} \quad (28)$$

Equation (28) describes the streamlines on a yawed cone to first order in the yaw parameter λ . The new coordinate x^2 runs from -1 at the top of the cone to +1 at the bottom.

The curves orthogonal to the streamlines are defined by

$$\frac{dr}{r \sin \Theta d\psi} = - \frac{ez \sin \psi}{u + ex \cos \psi}$$

which upon integration yields

$$x^1 = r(1 - \lambda \sin^2 \Theta \frac{z}{u} \cos \psi) \quad (29)$$

On the left of (29), x^1 is a parameter associated with the family of normal curves or, alternatively, a coordinate measured along the streamlines. Equations (28) and (29) are the transformation from the unyawed to the yawed coordinate system.

The inverse transformation is readily found to be

$$r = x^1(1 - \lambda \sin^2 \Theta \frac{z}{u} x^2) \quad (30)$$

$$\cos \psi = -x^2 - \lambda \left[1 - (x^2)^2 \right] \left\{ \frac{z}{u} \ln x^1 - \frac{x \sin \Theta}{2u} \ln \left[1 - (x^2)^2 \right] \right\} \quad (31)$$

On the surface,

$$\begin{aligned} (ds)^2 &= (dr)^2 + (r \sin \Theta d\psi)^2 \\ &= g_{11}(dx^1)^2 + g_{22}(dx^2)^2 \end{aligned} \quad (32)$$

Using (30) and (31) in (32), it is found that

$$g_{11} = 1 - 2\lambda \sin^2 \Theta \frac{z}{u} x^2 \quad (33)$$

$$g_{22} = \frac{(x^1 \sin \Theta)^2}{1 - (x^2)^2} \left(1 - 2\lambda x^2 \left\{ \frac{z}{u} \sin^2 \Theta + \frac{z}{u} \ln x^1 - \frac{x}{u} \sin \Theta - \frac{x}{u} \frac{\sin \Theta}{2} \ln [1 - (x^2)^2] \right\} \right) \quad (34)$$

The density and velocity at the edge of the boundary layer are also required in the equation of motion. They are obtained from reference 18 to first order in λ as follows:

$$u_s^2 = u^2 + w^2 = \bar{u}^2 (1 - 2\lambda \frac{x \sin \Theta}{\bar{u}} x^2) \quad (35)$$

$$\rho_s = \bar{\rho} (1 - \lambda \frac{\xi \sin \Theta}{\bar{\rho}} x^2) \quad (36)$$

$$p_s = \bar{p} (1 - \lambda \frac{\eta \sin \Theta}{\bar{p}} x^2) \quad (37)$$

From (35), (36), and (37), it follows that

$$T_s = \bar{T} \left[1 + \lambda \sin \Theta \left(\frac{\xi}{\bar{\rho}} - \frac{\eta}{\bar{p}} \right) x^2 \right] \quad (38)$$

and

$$M_s^2 = \bar{M}^2 \left[1 + \lambda \sin \Theta \left(\frac{\eta}{\bar{p}} - \frac{2x}{u} - \frac{\xi}{\bar{\rho}} \right) x^2 \right] \quad (39)$$

In the preceding equations, a bar over a quantity indicates its value at zero yaw.

With the aid of expressions developed, it is possible to show that, for a cone at small angle of yaw, the forms hypothesized for the velocity and density profiles in the preceding section are indeed appropriate. The substitution of (16), (33), (34), and (37) into the equation of motion (7) gives, upon neglecting terms of second order in α and λ and the term of order δ ,

$$\sum_{i=0}^2 \left[\rho u(i) \frac{\partial u(i)}{\partial s(i)} \right] = \frac{\partial \tau(01)}{\partial s(0)}$$

The pressure gradient is seen to be negligible, so that the velocity profiles (15) and (16) are good approximations.

Moreover, replacing $u(1)$ by temperature and $\tau(01)$ by heat flux over heat capacity in the preceding equation results in the energy equation. This is the condition necessary for Reynolds' analogy between stress and heat flux to hold. Consequently, the density (or temperature) profile (17), which is based on Reynolds' analogy, can be properly used for the cone at small angle of yaw.

SOLUTION OF THE MOMENTUM INTEGRAL EQUATIONS

The momentum integral equations (12) and (13) are now to be written for a yawed cone at constant temperature in terms of the boundary-layer thickness δ and the deflection angle α . In order to do this it is necessary to evaluate first the integrals (11) using (15) through (21). It is convenient to specialize at once to $n = 7$ in the profiles (15) and (16) and to make the following definitions:

$$I_m \equiv \int_0^1 \frac{\xi^m d\xi}{1 + \bar{B}\xi - \bar{A}^2\xi^2}$$

$$I_{m,2} \equiv \int_0^1 \frac{\xi^m d\xi}{(1 + \bar{B}\xi - \bar{A}^2\xi^2)^2}$$

$$= - \frac{1}{4\bar{A}^2 + \bar{B}^2} \left[\frac{\bar{B} - 2\bar{A}^2}{1 + \bar{B} - \bar{A}^2} + 2\bar{A}^2(m-1)I_m - \bar{B}mI_{m-1} \right]$$

$$\bar{A}^2 \equiv \text{Pr}^{1/3} \frac{\gamma-1}{2} \bar{M}^2 \frac{\bar{T}}{\bar{T}_w}$$

$$\bar{B} \equiv \frac{\bar{T}}{\bar{T}_w} \left(1 + \text{Pr}^{1/3} \frac{\gamma-1}{2} \bar{M}^2 \right) - 1$$

$$B_1 \equiv \frac{\bar{T}}{\bar{T}_w} \left[\frac{\xi}{\rho} - \frac{\eta}{p} - \frac{x}{u} \text{Pr}^{1/3} (\gamma-1) \bar{M}^2 \right]$$

Then to first order in λ and α , the displacement and momentum thicknesses (11) become

$$\left. \begin{aligned}
 \frac{\delta_1^*}{\delta} &= 1 - 7 \frac{\bar{T}}{T_w} I_7 + \lambda \sin \Theta \frac{\bar{T}}{T_w} \left[\left(\frac{\eta}{p} - \frac{\xi}{\rho} \right) I_7 + B_1 I_{8,2} + 2 \frac{\bar{x}}{u} \bar{A}^2 I_{9,2} \right] x^2 \\
 &\equiv L_0 + \lambda \sin \Theta L_1 x^2 \\
 \frac{\delta_2^*}{\delta} &= \alpha \frac{\bar{T}}{T_w} 7(I_7 - 2I_{14} + I_{21}) \\
 &\equiv \alpha N_1 \\
 \frac{\theta_{21}}{\delta} &= \alpha \frac{\bar{T}}{T_w} 7(I_8 - 2I_{15} + I_{22}) \\
 &\equiv \alpha P_1 \\
 \frac{\theta_{11}}{\delta} &= 7 \frac{\bar{T}}{T_w} (I_7 - I_8) + \lambda \sin \Theta 7 \frac{\bar{T}}{T_w} \left[\left(\frac{\xi}{\rho} - \frac{\eta}{p} \right) (I_7 - I_8) \right. \\
 &\quad \left. - B_1 (I_{8,2} - I_{9,2}) - 2 \frac{\bar{x}}{u} \bar{A}^2 (I_{9,2} - I_{10,2}) \right] x^2 \\
 &\equiv R_0 + \lambda \sin \Theta R_1 x^2 \\
 \frac{\theta_{22}}{\delta} &= \alpha'(\alpha^2)
 \end{aligned} \right\} (40)$$

The integrals I_7 , I_8 , and $(I_7 - I_8)$ appearing in (40) are listed in the tables of references 20 and 21. The integrals I_9 and I_{10} , which are required to compute $I_{9,2}$ and $I_{10,2}$, may be obtained from the recurrence relation

$$I_{m+1} = \frac{1}{A^2} \left(\bar{B} I_m + I_{m-1} - \frac{1}{m} \right)$$

The combinations of integrals $(I_7 - 2I_{14} + I_{21})$ and $(I_8 - 2I_{15} + I_{22})$ should be computed separately, rather than from the recurrence relation, to avoid cumulative error.

The Blasius formula (20) may likewise be expressed in terms of stream parameters at zero yaw. If a linear viscosity law is used,

$$\frac{\mu}{\mu_s} = C \frac{T}{T_s}$$

then (from (20))

$$C_F = K \left(\frac{\bar{T}}{\bar{T}_m} \right)^{1/2} \left(\frac{\bar{v}}{\bar{u}\delta} \right)^{1/4} (1 + \lambda F \sin \Theta x^2) \quad (41)$$

where

$$F = -\frac{1}{2} \frac{\bar{T}}{\bar{T}_m} \left[0.11 \text{Pr}^{1/3} (\gamma - 1) \bar{M}^2 \left(\frac{\eta}{p} - \frac{\xi}{\rho} - 2 \frac{x}{u} \right) - \frac{1}{2} \left(\frac{\xi}{\rho} - \frac{\eta}{p} \right) \frac{T_w}{\bar{T}} \right] \\ + \frac{1}{4} \left(2 \frac{\xi}{\rho} - \frac{\eta}{p} + \frac{x}{u} \right) \quad (42)$$

Introducing the thicknesses (40) and the friction coefficient (41) into the momentum integral equations (12) and (13) gives, to first order in α and λ ,

$$\frac{\partial}{\partial x^1} \delta (R_0 + \lambda \sin \Theta R_1 x^2) + \delta (R_0 + \lambda \sin \Theta R_1 x^2) \frac{1}{x^1} (1 - \lambda \frac{z}{u} x^2) \\ + \frac{\sqrt{1 - (x^2)^2}}{\sin \Theta x^1} [1 + \mathcal{O}(\lambda)] \left[\frac{\partial}{\partial x^2} N_1 \delta \alpha - N_1 \delta \alpha \mathcal{O}(\lambda) \right] \\ - \frac{\sqrt{1 - (x^2)^2}}{\sin \Theta x^1} [1 + \mathcal{O}(\lambda)] \left[\frac{\partial}{\partial x^2} P_1 \delta \alpha - P_1 \delta \alpha \mathcal{O}(\lambda) \right] \\ = K \left(\frac{\bar{T}}{\bar{T}_m} \right)^{1/2} \left(\frac{\bar{v}}{\bar{u}\delta} \right)^{1/4} \left[1 + \lambda \sin \Theta (F - \frac{z}{u} \sin \Theta) x^2 \right] \quad (43)$$

and

$$\frac{\partial}{\partial x^1} P_1 \delta \alpha + P_1 \delta \alpha \frac{2}{x^1} [1 + (\lambda)] \\ - \delta [R_0 + L_0 + \lambda \sin \Theta (R_1 + L_1) x^2] \lambda \sin \Theta \frac{z}{u} \frac{\sqrt{1 - (x^2)^2}}{x^1} \\ = \alpha K \left(\frac{\bar{T}}{\bar{T}_m} \right)^{1/2} \left(\frac{\bar{v}}{\bar{u}\delta} \right)^{1/4} [1 + \mathcal{O}(\lambda)] \quad (44)$$

In order to solve (43) and (44), the dependent variables α and δ are expanded in powers of (small) yaw parameter λ :

$$\left. \begin{aligned} \tan \alpha &= \alpha_1 \lambda + \alpha_2 \lambda^2 + \dots \\ \delta &= \delta_0 + \delta_1 \lambda + \dots \end{aligned} \right\} \quad (45)$$

Equation (43) yields equations of zero and first order in λ , and (44) yields a first-order equation as follows:

$$\frac{\partial \delta_0}{\partial x^1} + \frac{\delta_0}{x^1} = \frac{K}{R_0} \left(\frac{\bar{T}}{\bar{T}_m} \right)^{1/2} \left(\frac{\bar{v}}{\bar{u} \delta_0} \right)^{1/4} \quad (46)$$

$$\begin{aligned} \frac{\partial \delta_1}{\partial x^1} + \frac{\delta_1}{x^1} + \frac{K}{4R_0} \left(\frac{\bar{T}}{\bar{T}_m} \right)^{1/2} \left(\frac{\bar{v}}{\bar{u} \delta_0} \right)^{1/4} \frac{\delta_1}{\delta_0} \\ = -\sin \Theta \frac{R_1}{R_0} \frac{\partial \delta_0}{\partial x^1} x^2 + \delta_0 \left(\frac{z}{u} - \sin \Theta \frac{R_1}{R_0} \right) \frac{x^2}{x^1} \\ + K \left(\frac{\bar{T}}{\bar{T}_m} \right)^{1/2} \left(\frac{\bar{v}}{\bar{u} \delta_0} \right)^{1/4} \sin \Theta \left(\frac{F - \frac{z}{u} \sin \Theta}{R_0} \right) x^2 \\ + \frac{\sqrt{1 - (x^2)^2}}{x^1 \sin \Theta} \delta_0 \frac{\partial \alpha_1}{\partial x^2} \left(\frac{P_1 - N_1}{R_0} \right) \end{aligned} \quad (47)$$

$$\begin{aligned} \frac{\partial}{\partial x^1} \delta_0 \alpha_1 + 2 \frac{\delta_0 \alpha_1}{x^1} = \frac{z}{u} \frac{\sin \Theta}{P_1} (L_0 + R_0) \delta_0 \frac{\sqrt{1 - (x^2)^2}}{x^1} \\ - \frac{K}{P_1} \left(\frac{\bar{T}}{\bar{T}_m} \right)^{1/2} \left(\frac{\bar{v}}{\bar{u} \delta_0} \right)^{1/4} \alpha_1 \end{aligned} \quad (48)$$

Equation (46) is simply the integral equation for the unyawed cone. The solution of (46) satisfying the condition $\delta(x^1 = 0) = 0$ is

$$\frac{\bar{u} \delta_0}{\bar{v}} = \left(\frac{\bar{T}}{\bar{T}_m} \right)^{2/5} \left(\frac{5K}{9R_0} \frac{\bar{u} x^1}{\bar{v}} \right)^{4/5} \quad (49)$$

Substitution of (49) into (48) yields

$$\alpha_1 = \sin \Theta \frac{z}{u} \left(\frac{L_0 + R_0}{14P_1 + 9R_0} \right) \sqrt{1 - (x^2)^2} \quad (50)$$

Then using (49) and (50), the solution of (47) is found to be

$$\begin{aligned} \frac{\bar{u}\delta_1}{\bar{v}} &= \frac{4}{9} \left[\frac{9}{5} \sin \Theta \left(F - \frac{z}{u} \sin \Theta - \frac{R_1}{R_0} \right) + \frac{z}{u} \right. \\ &\quad \left. + 5 \frac{z}{u} \frac{N_1 - P_1}{R_0} \frac{L_0 + R_0}{14P_1 + 9R_0} \right] \left(\frac{\bar{T}}{\bar{T}_m} \right)^{2/5} \left(\frac{5K}{9R_0} \frac{\bar{u}x^1}{\bar{v}} \right)^{4/5} x^2 \\ &\equiv \frac{4}{9} D \left(\frac{\bar{T}}{\bar{T}_m} \right)^{2/5} \left(\frac{5K}{9R_0} \frac{\bar{u}x^1}{\bar{v}} \right)^{4/5} x^2 \end{aligned} \quad (51)$$

Equations (50) and (51) show that the boundary-layer thickness has its greatest changes at the windward and leeward rays of the cone and that the fluid in the boundary layer is deflected most in the horizontal plane (fig. 1).

BOUNDARY-LAYER EFFECTS

From the results of the previous section it is possible to find the effect of the boundary layer on the outer stream and the forces it exerts on the body.

Displacement Surface

Let $\Delta(x^1, x^2)$ designate the distance, in the normal direction from the body surface, which the potential flow is displaced by the boundary layer. Moore (ref. 22) has shown that Δ is determined by

$$\text{div} \left[\rho_s \vec{u}_s \Delta - \int_0^\delta (\rho_s \vec{u}_s - \rho \vec{u}) ds(0) \right] = 0 \quad (52)$$

where the arrows designate vector quantities. In terms of the previously defined boundary-layer thicknesses, (52) becomes

$$\frac{\partial}{\partial x^1} \rho_s u_s \sqrt{g_{22}} (\Delta - \delta_1^*) = \frac{\partial}{\partial x^2} \rho_s u_s \sqrt{g_{11}} \delta_2^* \quad (53)$$

Equation (53) and the boundary condition at the tip show that, on the unyawed cone, the surface Δ has the value of the usual displacement thickness δ_1^* . Substitution of (33) through (36), (40), (49), (50), and (51) into (53) yields

$$\frac{\Delta}{L_0 \delta_0} = 1 + \lambda x^2 \left(\frac{4}{9} D + \frac{L_1}{L_0} \sin \Theta + \frac{25}{9} \frac{z}{u} \frac{N_1}{L_0} \frac{L_0 + R_0}{14P_1 + 9R_0} \right) \quad (54)$$

For a positive value of the yaw parameter λ , Δ is nearly a circular cone whose axis is inclined downward from that of the body.

Local Friction Coefficient

Because Reynolds' analogy shows that the local friction coefficient is proportional to the local heat-transfer coefficient, it is desirable to know the local distribution of stresses on the surface of the cone as well as the net forces. Combining (29), (41), (45), (49), and (51) yields the friction coefficient:

$$C_f = K \left(\frac{\bar{T}}{\bar{T}_m} \right)^{1/2} \left[\frac{5K}{9R_0} \left(\frac{\bar{T}}{\bar{T}_m} \right)^{1/2} \frac{\bar{u}r}{\bar{v}} \right]^{-1/5} \left[1 - \lambda \left(F \sin \Theta - \frac{1}{9} D - \frac{1}{5} \sin^2 \Theta \frac{z}{u} \right) \cos \psi \right]$$

$$\equiv \bar{C}_f \left[1 - \lambda \left(F \sin \Theta - \frac{1}{9} D - \frac{1}{5} \sin^2 \Theta \frac{z}{u} \right) \cos \psi \right] \quad (55)$$

Using as a measure of heat transfer the Stanton number,

$$St \equiv \frac{q_w}{c_p (\bar{T}_{w0} - T_w) \rho u}$$

where q_w is the heat transferred at the wall, c_p is the heat capacity, and \bar{T}_{w0} is the insulated wall temperature, then

$$St = \frac{1}{2} C_f$$

Frictional Drag Force

For the net forces on the cone it is convenient to transform the stresses from the streamline system of coordinates (x-system) to the body system (r, ψ , y, fig. 1). The transformations required are

$$\left. \begin{aligned} \tau_{(yr)} &= \tau_{(01)} \left(\frac{\partial x^1}{\partial r} \sqrt{g_{11}} + \lambda \alpha_1 \frac{\partial x^2}{\partial r} \sqrt{g_{22}} \right) \\ \tau_{(y\psi)} &= \frac{1}{r \sin \Theta} \tau_{(01)} \left(\frac{\partial x^1}{\partial \psi} \sqrt{g_{11}} + \lambda \alpha_1 \frac{\partial x^2}{\partial \psi} \sqrt{g_{22}} \right) \end{aligned} \right\} \quad (56)$$

from which

$$\left. \begin{aligned} \tau(yr) &= \tau(01) [1 + \sigma(\lambda^2)] \\ \tau(y\psi) &= \lambda \tau(01) \sin \psi \frac{z}{u} \sin \Theta \left(1 + 5 \frac{R_0 + L_0}{14P_1 + 9R_0} \right) \end{aligned} \right\} \quad (57)$$

The force on an element of area da^j on the cone surface is

$$dF_i = \tau_{ij} da^j$$

The net force in the direction of any unit vector \vec{v} is

$$F(v) = \int \tau_{ij} v^i da^j \quad (58)$$

If \vec{v} is in the direction of the cone axis, it has no ψ -component, and the drag force is

$$F_D = 2 \cos \Theta \sin \Theta \int_0^r \int_0^\pi \tau(yr) r dr d\psi$$

The viscous stress appearing in the integral is, by (12) and (57),

$$\tau(yr) = \bar{\tau}(01) \left\{ 1 - \lambda \cos \psi \left[\sin \Theta F - \frac{1}{9} D - \frac{1}{5} \sin^2 \Theta \frac{z}{u} - \sin \Theta \left(2 \frac{x}{u} + \frac{\xi}{\rho} \right) \right] \right\} \quad (59)$$

The frictional drag coefficient is then

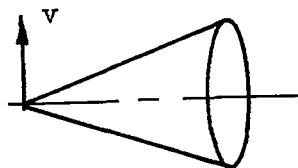
$$\begin{aligned} C_D &\equiv \frac{F_D}{\rho u^2 \pi r^2 \sin \Theta} \\ &= \frac{10}{9} (\cos \Theta) K \left(\frac{\bar{T}}{\bar{T}_m} \right)^{1/2} \left[\frac{5K}{9R_0} \left(\frac{\bar{T}}{\bar{T}_m} \right)^{1/2} \left(\frac{ur}{\bar{v}} \right) \right]^{-1/5} [1 + \sigma(\lambda^2)] \end{aligned} \quad (60)$$

To first order, there is no change in the drag coefficient with yaw.

Comparison with the pressure-drag coefficients of reference 18 reveals that the pressure forces are of the order of a hundred times the frictional forces.

Frictional Lift Force

Consider the force in the direction of unit vector \vec{v} in the plane of yaw and perpendicular to the axis.



The components of \vec{v} are

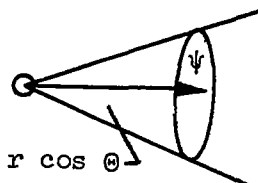
$$(v_r, v_\psi, v_y) = (\sin \Theta \cos \psi, -\sin \psi, \cos \Theta \cos \psi) \quad (61)$$

Combination of (57), (58), (60), and (61) yields for the ratio of the frictional lift force to the frictional drag force

$$\frac{F_L}{F_D} \equiv \frac{C_L}{C_D} = -\lambda \frac{\tan \Theta}{2} \left\{ \left[F \sin \Theta - \frac{1}{9} D - \frac{1}{5} \sin^2 \Theta \frac{z}{u} - \sin \Theta \left(2 \frac{x}{u} + \frac{\xi}{\rho} \right) \right] + \frac{z}{u} \left(1 + 5 \frac{R_0 + L_0}{14P_1 + 9R_0} \right) \right\} \quad (62)$$

Frictional Pitching Moment

Consider the moment of forces about an axis through the cone apex, normal to the plane of yaw. The stress $\tau(ry)$ acts through the apex and



so cannot contribute to the moment. The stress $\tau(\psi y)$ has a moment arm $r \cos \Theta$, and its component in the upward direction is

$$-\sin \psi \tau(\psi y)$$

The pitching moment is then

$$\mathcal{M} = -2 \sin \Theta \cos \Theta \int_0^r \int_0^\pi \sin \psi \tau(\psi y) r^2 dr d\psi$$

Use of equations (57) and (60) results in

$$C_M = \frac{\mathcal{M}}{F_D r \cos \Theta} = -\lambda \frac{9}{28} \tan \Theta \frac{z}{u} \left(1 + 5 \frac{R_0 + L_0}{14P_1 + 9R_0} \right) \quad (63)$$

for the frictional pitching moment.

NUMERICAL EXAMPLES

Computations of the boundary layer on the yawed cone have been made over a free-stream Mach number range of 1 to 4 to show the effect of cone angle and temperature ratio. The Prandtl number was taken as 0.7.

The computational procedure is as follows. For a given Mach number and cone angle, the parameters \bar{u} , x , z , ξ/ρ , and η/\bar{p} are obtained from reference 18. For a given Mach number and temperature ratio, the integrals I_7 and I_8 are obtained from reference 20 or 21. The integrals I_9 and I_{10} are obtained from I_7 and I_8 by the recursion formula. The combinations of integrals $(I_7 - 2I_{14} + I_{21})$ and $(I_8 - 2I_{15} + I_{22})$ are functions of \bar{M} (zero yaw Mach number on the cone surface) and the temperature ratio \bar{T}/T_w . They are plotted in figure 2, which shows that they are nearly linear in \bar{M}^2 . From these parameters and integrals, the quantities L_0 , L_1 , R_0 , R_1 , P_1 , and N_1 (eq. (40)) may be obtained, and with them the coefficients of the previous section.

In figure 3 is shown the parameter (from eq. (54))

$$-\frac{1}{\cos \psi} \left[\frac{\partial \Delta}{\partial \lambda} \right]_{\lambda=0} = \frac{4}{9} D + \frac{L_1}{L_0} \sin \Theta + \frac{25}{9} \frac{z}{u} \frac{N_1}{L_0} \frac{L_0 + R_0}{14P_1 + 9R_0}$$

which determines the deflection of the displacement surface axis from the cone axis. Figure 3(a) shows the effect of temperature ratio on a 20° cone, and figure 3(b) shows the effect of cone angle at constant temperature ratio. A comparison with the displacement surface of a laminar adiabatic boundary layer (ref. 3) is made. The parameter is of the same order of magnitude for the two boundary layers over the Mach number range considered, although slightly higher for the laminar flow. The displacement surface deflection is slightly greater for low wall temperatures because of the increased density in the boundary layer.

The deflection of the inner streamline is determined by the parameter (eq. (50))

$$\frac{\alpha_1}{\sin \psi} = \sin \Theta \frac{z}{u} \left(\frac{L_0 + R_0}{14P_1 + 9R_0} \right)$$

Figure 4 shows that the deflection is considerably less in the turbulent boundary layer than in the laminar. The fluid in the laminar layer, having less kinetic energy, is influenced more by the transverse pressure gradient. Figure 4(a) shows the effect of temperature ratio, and figure 4(b) shows the effect of cone angle. When the wall temperature is high, the density in the boundary layer is lowered, and greater deflection results.

The change in local skin-friction coefficient $\tau(01)/\rho_s u_s^2$ with yaw is determined by (eq. (35))

$$-\left. \frac{1}{C_f \cos \psi} \frac{\partial C_f}{\partial \lambda} \right]_{\lambda=0} = F \sin \Theta - \frac{1}{9} D - \frac{1}{5} \sin^2 \Theta \frac{z}{u}$$

Figure 5, a plot of this quantity, shows that the effect of temperature ratio is small, whereas the effect of cone angle is appreciable. The comparison with the laminar flow again reveals that the turbulent boundary layer is less affected by yaw.

The viscous lift coefficient (eq. (62)) is shown in figure 6. There are two types of forces contributing to this coefficient. The viscous shear is greater on the top of the yawed cone than on the bottom, resulting in a lift force in the direction of yaw. The circumferential forces always give a lift force opposing yaw. For small-angle cones the drag forces grow relatively larger with Mach number until finally the resultant lift is in the direction of yaw.

The pitching moment is shown in figure 7. It is proportional to that part of the lift caused by the circumferential forces. It is slightly higher for the higher ratios T_w/\bar{T} because of the greater deflection of the low-density fluid in the boundary layer.

CONCLUDING REMARKS

The over-all picture given by the foregoing computations is that the turbulent boundary layer on the yawed cone behaves qualitatively like the laminar layer, but the relative magnitude of the effect is always less. Thus, the deflection of the fluid in the boundary layer, the frictional lift, and the frictional pitching are relatively smaller because of the higher shear stresses.

The assumptions entering into the formulation of the problem should be kept in mind in interpreting the results. The assumption that the skin-friction law for plane flow holds for flows with slightly curved streamlines should not be far from the true picture. The choice of a power-law profile for the velocity component in direction of the outer stream is considered reasonable because the pressure gradients are small. But the selection of the proper profile for the transverse component is less certain and at the same time critical, for it is this profile that determines the three-dimensional effects. The results presented here give magnitudes and general trends, but are not necessarily quantitatively accurate.

The analysis gives no information about the separation of the boundary layer. It is limited to small perturbations, from zero yaw, of the potential stream; consequently, there are no strong pressure gradients to induce separation. Any form factor constructed from ratios of the boundary-layer thicknesses varies at most to order λ over the cone surface, whereas separation is associated with the growth of a form factor to some large critical value.

Lewis Flight Propulsion Laboratory
National Advisory Committee for Aeronautics
Cleveland, Ohio, October 24, 1957

APPENDIX - SELECTION OF DOMINANT STRESS TERMS

The turbulent stresses arise in equation (2) in the covariant derivative $\tau_{l,l}^i$. In a plane flow the normal stresses $\tau_0^0, \tau_1^1, \tau_2^2$ and the shear stresses τ_1^0, τ_0^1 are known from experimental measurement to be of the same order of magnitude. In three-dimensional boundary layers, additional stresses $\tau_0^2, \tau_1^2, \tau_2^0, \tau_2^1$ arise that may be smaller, but certainly no larger, than the normal stresses.

In the x^1 equation of motion the stress terms are

$$\begin{aligned} & \frac{1}{g_{00}} \tau_{0,0}^1 + \frac{1}{g_{11}} \tau_{1,1}^1 + \frac{1}{g_{22}} \tau_{2,2}^1 \\ & \equiv \frac{1}{g_{00}} \left(\frac{\partial \tau_0^1}{\partial x^0} + \Gamma_{10}^1 \tau_0^1 - \Gamma_{00}^1 \tau_1^1 \right) + \frac{1}{g_{11}} \left(\frac{\partial \tau_1^1}{\partial x^1} + \Gamma_{11}^1 \tau_1^1 - \Gamma_{11}^1 \tau_1^1 \right) \\ & + \frac{1}{g_{22}} \left(\frac{\partial \tau_2^1}{\partial x^2} + \Gamma_{12}^1 \tau_2^1 - \Gamma_{22}^1 \tau_1^1 \right) \end{aligned} \quad (A1)$$

where it is understood that i is summed from 0 to 2. The Γ_{mn}^l are the Christoffel symbols:

$$\Gamma_{mn}^l = 0 \quad \text{for} \quad l \neq m \neq n \neq l \quad (A2)$$

Also,

$$\Gamma_{00}^1 = \Gamma_{00}^2 = 0 \quad \text{and} \quad g_{00} = 1 \quad (A3)$$

Using (A2) and (A3), the right side of (A1) becomes

$$\begin{aligned} & \frac{\partial \tau_0^1}{\partial x^0} + \frac{1}{g_{11}} \frac{\partial \tau_1^1}{\partial x^1} + \frac{1}{g_{22}} \frac{\partial \tau_2^1}{\partial x^2} + \tau_1^0 \frac{1}{g_{11}} \Gamma_{01}^1 + \tau_0^1 \left(\Gamma_{10}^1 - \frac{1}{g_{11}} \Gamma_{11}^0 - \frac{1}{g_{22}} \Gamma_{22}^0 \right) \\ & - \tau_1^1 \frac{1}{g_{22}} \Gamma_{22}^1 + \tau_2^1 \left(-\frac{1}{g_{11}} \Gamma_{11}^2 + \frac{1}{g_{22}} \Gamma_{12}^1 - \frac{1}{g_{22}} \Gamma_{22}^2 \right) \\ & + \tau_1^2 \frac{1}{g_{11}} \Gamma_{21}^1 + \tau_2^2 \frac{1}{g_{22}} \Gamma_{22}^1 \end{aligned} \quad (A4)$$

Consider first the partial derivatives in (A4). They may be written in terms of the physical components and arc lengths,

$$\frac{1}{\sqrt{g_{11}}} \left[\frac{\partial \tau(10)}{\partial s(0)} + \frac{\partial \tau(11)}{\partial s(1)} + \frac{\partial \tau(12)}{\partial s(2)} \right] \quad (A5)$$

In a boundary layer, the stresses vary rapidly in the direction normal to the surface, but slowly in directions parallel to it. Thus, $\frac{\partial}{\partial s(0)} \sim \frac{1}{\delta}$, while $\frac{\partial}{\partial s(1)}$ and $\frac{\partial}{\partial s(2)} \sim \frac{1}{\Delta s}$, where Δs is a distance, measured on the surface, over which a stress varies an appreciable part of its total magnitude. Then,

$$\frac{\partial \tau(10)}{\partial s(0)} / \frac{\partial \tau(11)}{\partial s(1)}, \frac{\partial \tau(10)}{\partial s(0)} / \frac{\partial \tau(12)}{\partial s(2)} \sim \frac{\Delta s}{\delta} \gg 1 \quad (A6)$$

The Christoffel symbols are composed of terms of the form

$$\frac{1}{g_{mm}} \frac{\partial g_{mm}}{\partial x^n} = \frac{\partial}{\partial x^n} \ln g_{mm}$$

Therefore, to take a typical term as an example,

$$\begin{aligned} \tau_1^2 \frac{1}{g_{11}} \Gamma_{21}^1 &\sim \frac{1}{\sqrt{g_{11}}} \tau(21) \frac{\partial \ln g_{11}}{\partial s(2)} \\ &\sim \frac{1}{\sqrt{g_{11}}} \frac{\tau(21)}{\Delta s} \end{aligned} \quad (A7)$$

Consequently,

$$\frac{1}{\sqrt{g_{11}}} \frac{\frac{\partial \tau(10)}{\partial s(0)}}{\tau_1^2} \frac{1}{g_{11}} \Gamma_{21}^1 \sim \frac{\Delta s}{\delta} \gg 1$$

Thus all terms not involving derivatives of the stresses may be neglected. (The fact that some of the derivatives in the Christoffel symbols are taken with respect to x^0 does not make them large, for the g_{ij} are nearly constant through the boundary layer.)

It is seen that the only stress term which remains in the x^1 equation of motion is

$$\frac{1}{\sqrt{g_{11}}} \frac{\partial \tau(10)}{\partial s(0)}$$

A similar argument shows that in the x^2 equation of motion the only term of importance is

$$\frac{1}{\sqrt{g_{22}}} \frac{\partial \tau(20)}{\partial s(0)}$$

REFERENCES

1. Mangler, W.: Zusammenhang zwischen ebener und rotationssymmetrischer Grenzschichten in kompressiblen Flüssigkeiten. Z.a.M.M., Bd. 28, Apr. 1948, pp. 97-108.
2. Hantsche, W., and Wendt, H.: The Laminar Boundary Layer on a Circular Cone at Zero Incidence in a Supersonic Stream. Rep. and Trans. No. 276, British M.O.S., Aug. 1946.
3. Moore, Franklin K.: Laminar Boundary Layer on Circular Cone in Supersonic Flow at Small Angle of Attack. NACA TN 2521, 1951.
4. Moore, Franklin K.: Laminar Boundary Layer on Cone in Supersonic Flow at Large Angle of Attack. NACA Rep. 1132, 1953. (Supersedes NACA TN 2844.)
5. Illingworth, C. R.: The Laminar Boundary Layer on a Rotating Body of Revolution. Phil. Magazine, ser. 7, vol. 44, no. 351, Apr. 1953, pp. 389-403.
6. Feibig, Martin: Laminar Boundary Layer on Spinning Circular Cone in Supersonic Flow at a Small Angle of Attack. TN 56-532, Graduate School Aero. Eng., Cornell Univ., June 1956. (Office Sci. Res. Contract AF-18(600)-1523.)
7. Sedney, R.: Laminar Boundary Layer on a Spinning Cone at Small Angles of Attack. Rep. 991, Ballistics Res. Lab., Aberdeen Proving Ground, Sept. 1956.
8. Van Driest, E. R.: Turbulent Boundary Layer on a Cone in a Supersonic Flow at Zero Angle of Attack. Jour. Aero. Sci., vol. 19, no. 1, Jan. 1952, pp. 55-57; 72.
9. Gazley, C., Jr.: Theoretical Evaluation of the Turbulent Skin Friction and Heat Transfer on a Cone in Supersonic Flight. Rep. R49A0524, General Electric Co., Nov. 1949. (Proj. Hermes (TUL-2000A) U.S. Army Ord.)

10. Moore, Franklin K.: Three-Dimensional Boundary Layer Theory. Vol. IV of Advances in Appl. Mech., Academic Press, Inc., 1956, pp. 159-228.
11. Mager, Artur: Generalization of Boundary-Layer Momentum-Integral Equations to Three-Dimensional Flows Including Those of Rotating Systems. NACA Rep. 1067, 1952. (Supersedes NACA TN 2310.)
12. Michal, Aristotle D.: Matrix and Tensor Calculus. John Wiley & Sons, Inc., 1947.
13. Timman, R.: A Calculation Method for Three-Dimensional Laminar Boundary Layers. F.66, Nat. Luchtvaartlaboratorium (Amsterdam), Aug. 24, 1950.
14. Mager, Artur: Incompressible Non-Meridional Boundary Layer Flow on Bodies of Revolution. NAVORD Rep. 3366, 1953-1954, U.S. Naval Ord. Test Station, Sept. 13, 1954.
15. Tucker, Maurice: Approximate Turbulent Boundary-Layer Development in Plane Compressible Flow Along Thermally Insulated Surfaces with Application to Supersonic-Tunnel Contour Correction. NACA TN 2045, 1950.
16. Monaghan, R. J.: A Review and Assessment of Various Formulae for Turbulent Skin Friction in Compressible Flow. C.P. 142, British ARC, 1953.
17. Eckert, Ernst R. G.: Survey on Heat Transfer at High Speeds. Tech. Rep. 54-70, Aero. Res. Lab., Wright Air Dev. Center, Wright-Patterson Air Force Base, Apr. 1954.
18. The Staff of the Computing Section, Center of Analysis: Tables of Supersonic Flow Around Cones. Tech. Rep. No. 1; Tables of Supersonic Flow Around Yawing Cones, Tech. Rep. No. 3, Dept. Elec. Eng., M.I.T., 1947.
19. Van Dyke, Milton D., Young, George B. W., and Siska, Charles: Proper Use of the M.I.T. Tables for Supersonic Flow Past Inclined Cones. Jour. Aero. Sci., vol. 18, no. 5, May 1951, pp. 355-356.
20. Bartz, D. R.: An Approximate Solution of Compressible Turbulent Boundary-Layer Development and Convective Heat Transfer in Convergent-Divergent Nozzles. Trans. ASME, vol. 77, no. 8, Nov. 1955, pp. 1235-1245.
21. Mirels, Harold: Boundary Layer Behind Shock or Thin Expansion Wave Moving into Stationary Fluid. NACA TN 3712, 1956.
22. Moore, Franklin K.: Displacement Effect of a Three-Dimensional Boundary Layer. NACA Rep. 1124, 1953. (Supersedes NACA TN 2722.)

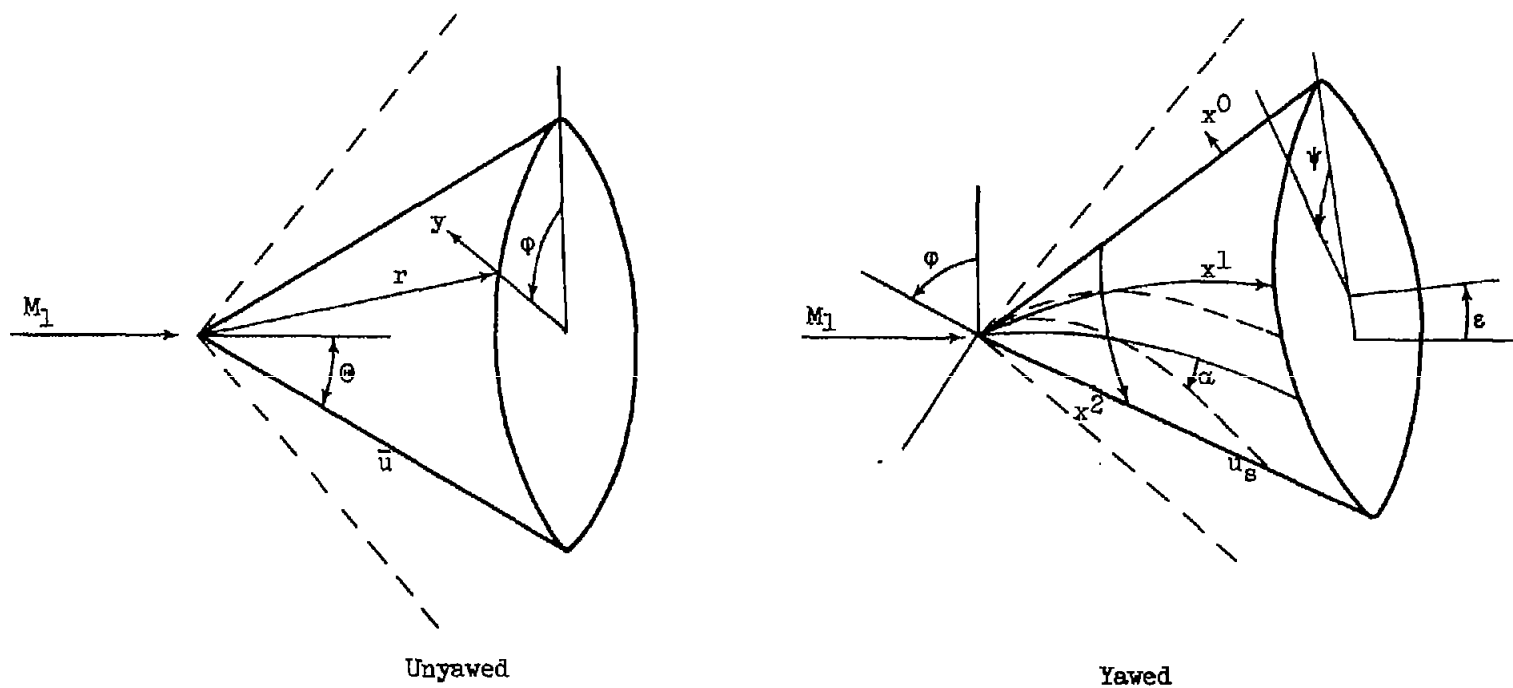


Figure 1. - Coordinate systems on unyawed and yawed cones.

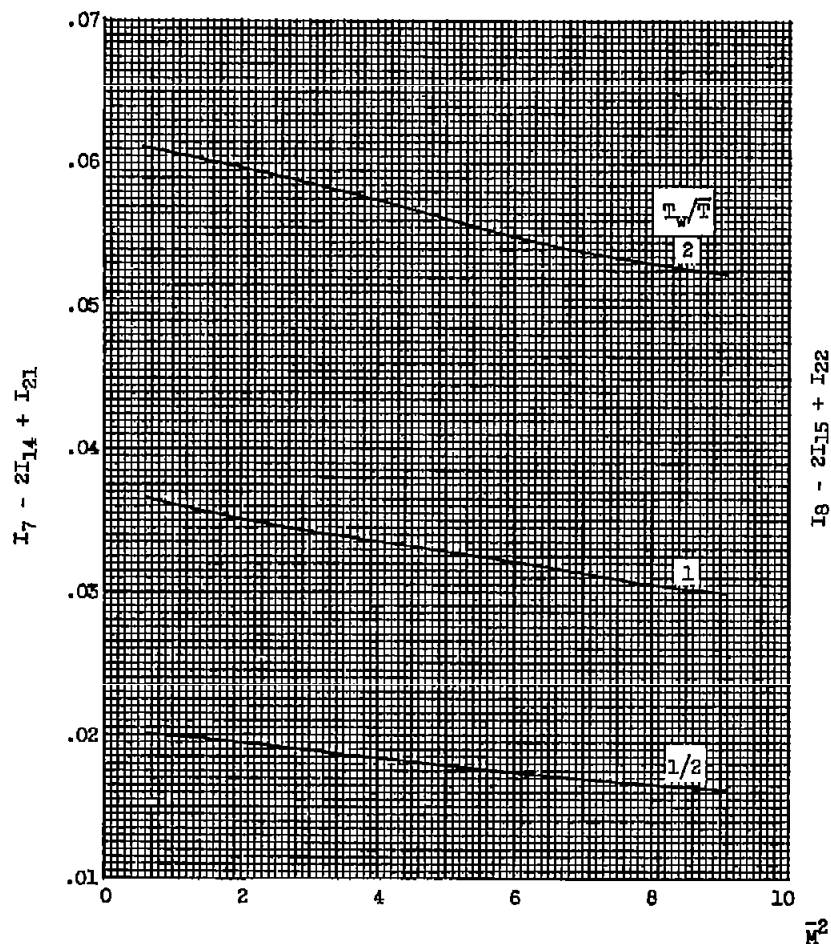
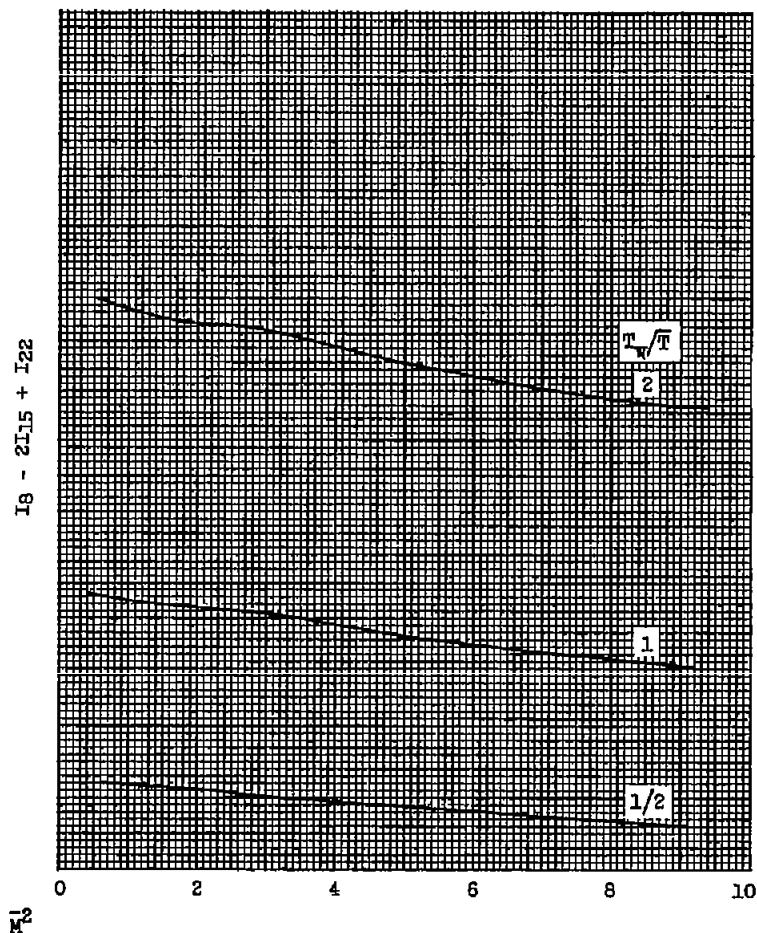
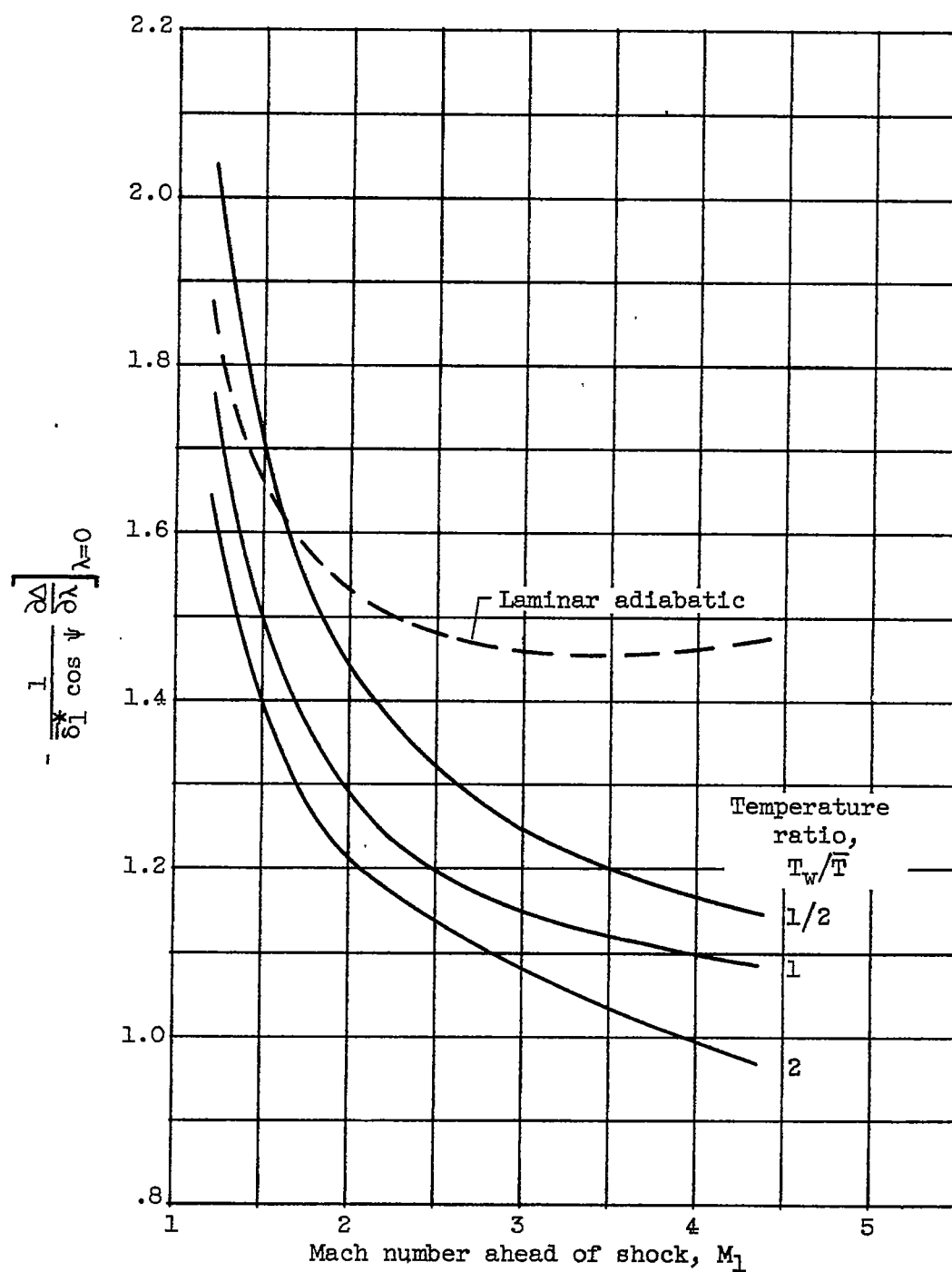
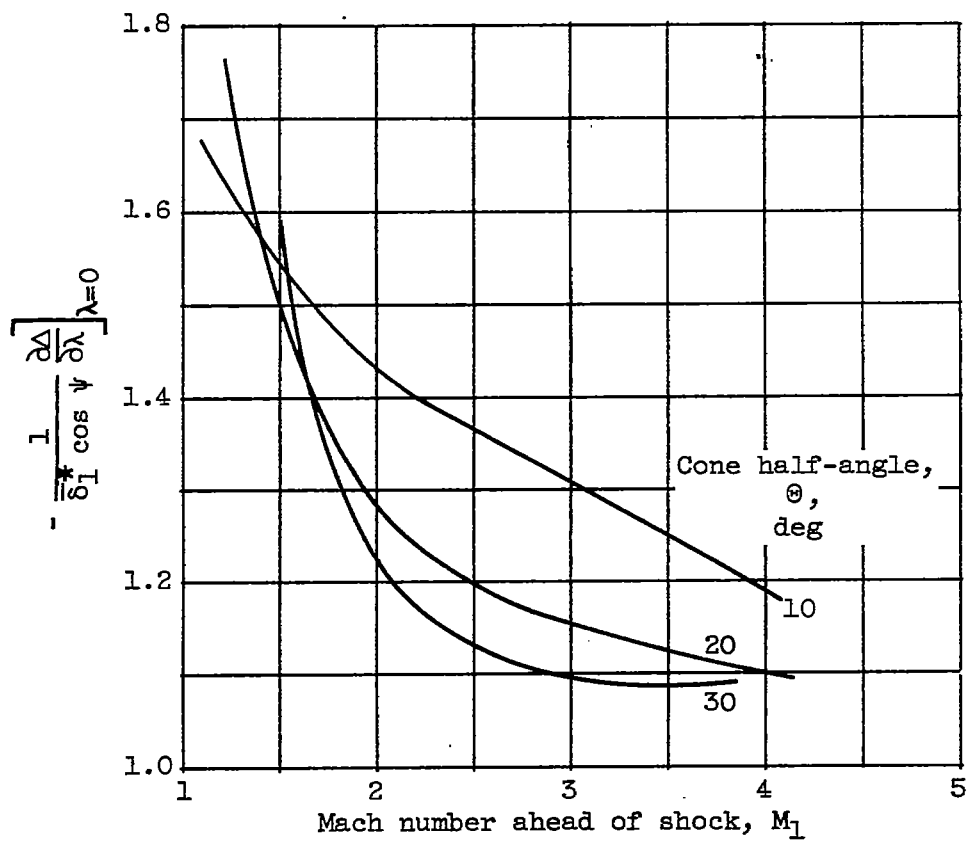
(a) Integrals arising in δ_2^* .(b) Integrals arising in θ_{21} .

Figure 2. - Integrals arising in boundary-layer thicknesses.



(a) Cone half-angle, 20° .

Figure 3. - Displacement surface parameter.



(b) Temperature ratio, T_w/\bar{T} , 1.

Figure 3. - Concluded. Displacement surface parameter.

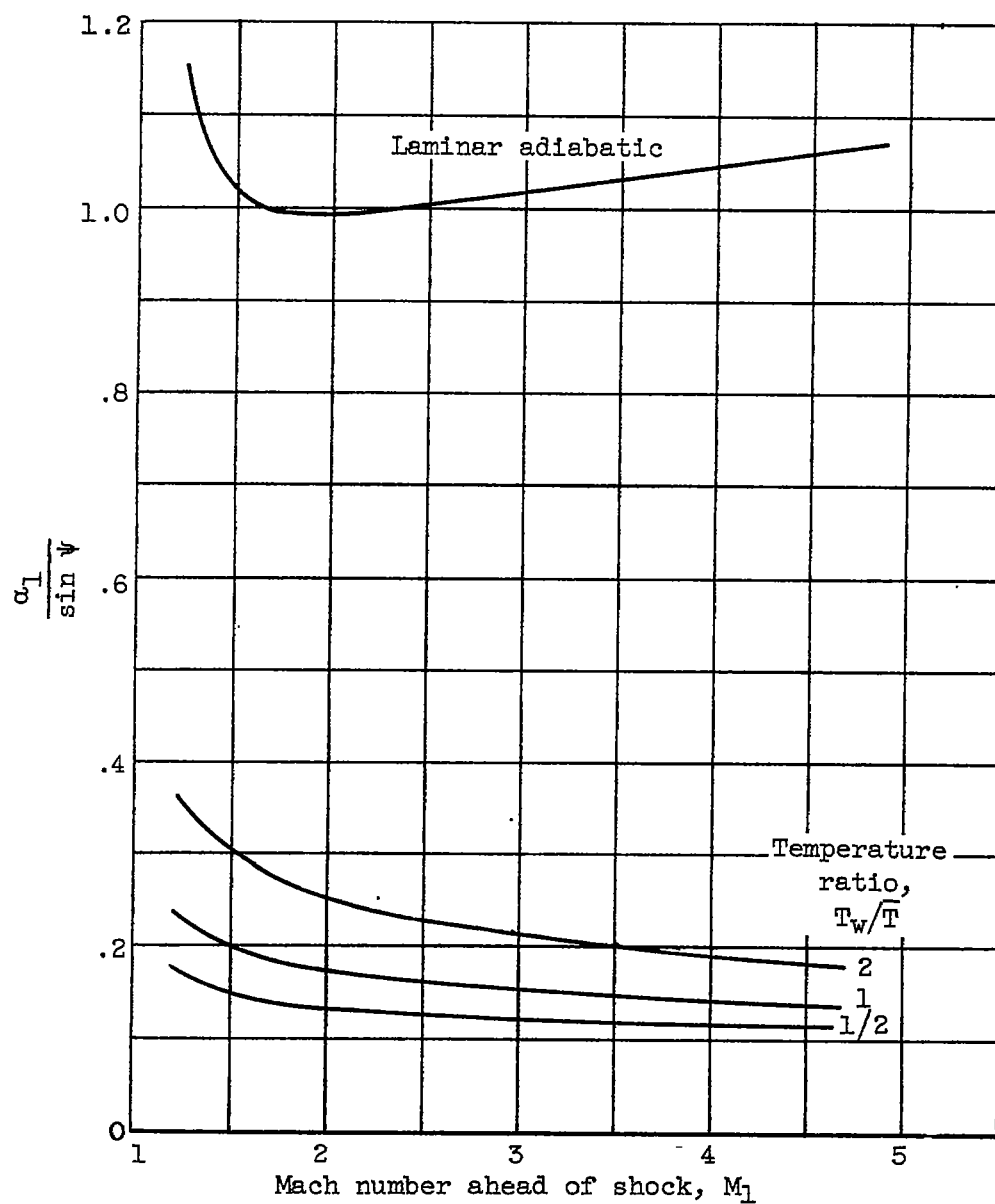
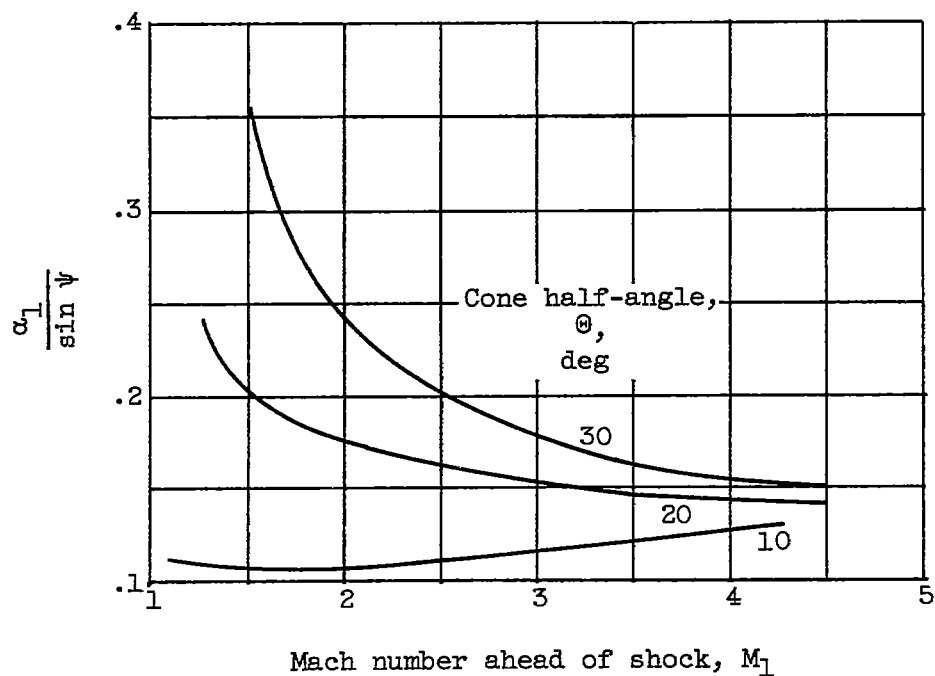
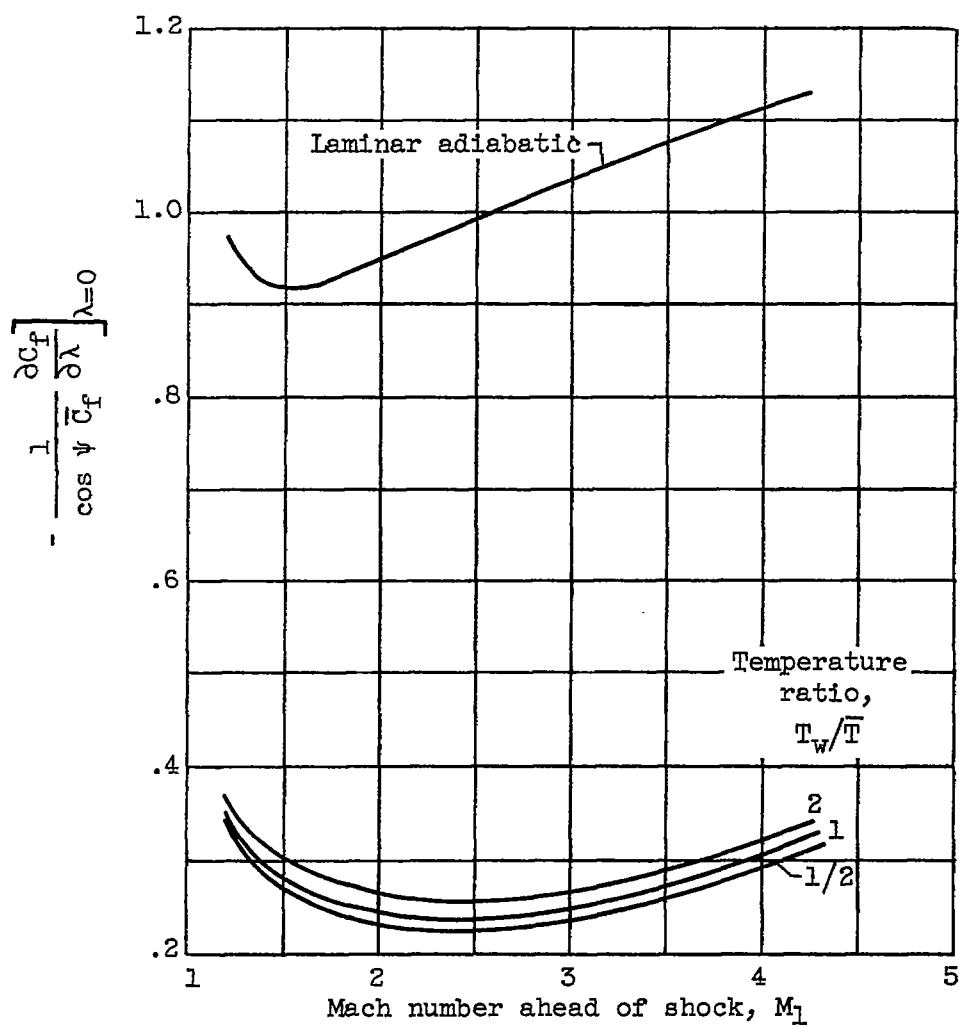
(a) Cone half-angle, 20° .

Figure 4. - Deflection of limiting streamline at surface with respect to potential-flow streamlines.



(b) Temperature ratio, T_w/\bar{T} , 1.

Figure 4. - Concluded. Deflection of limiting streamline at surface with respect to potential-flow streamlines.



(a) Cone half-angle, 20° .

Figure 5. - Local skin-friction coefficient.

4372

CP-5 back

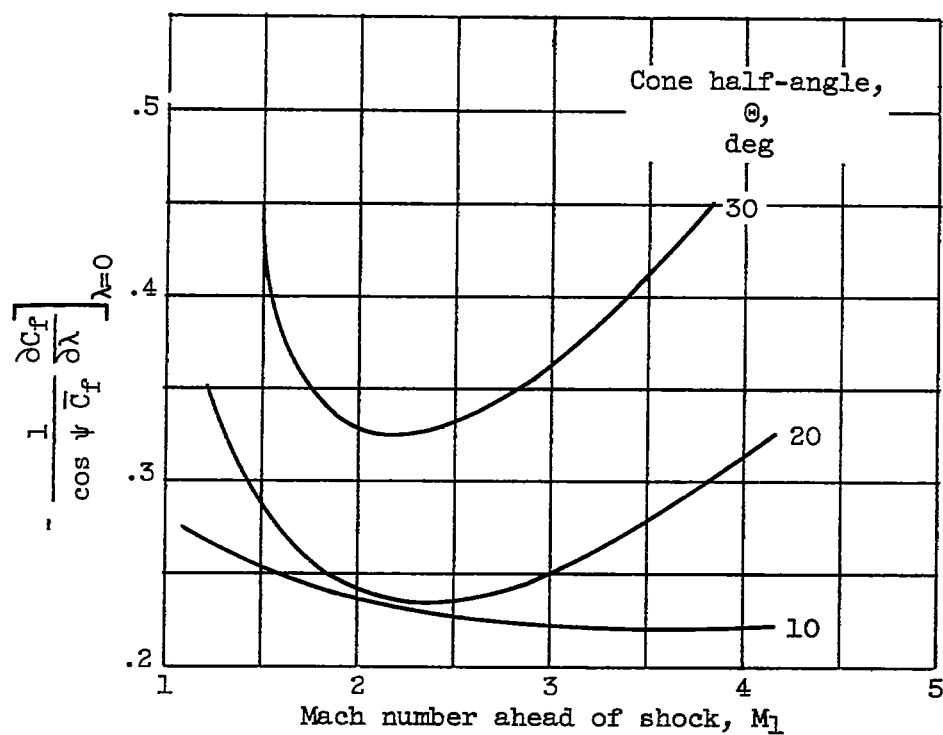
(b) Temperature ratio, T_w/\bar{T} , 1.

Figure 5. - Concluded. Local skin-friction coefficient.

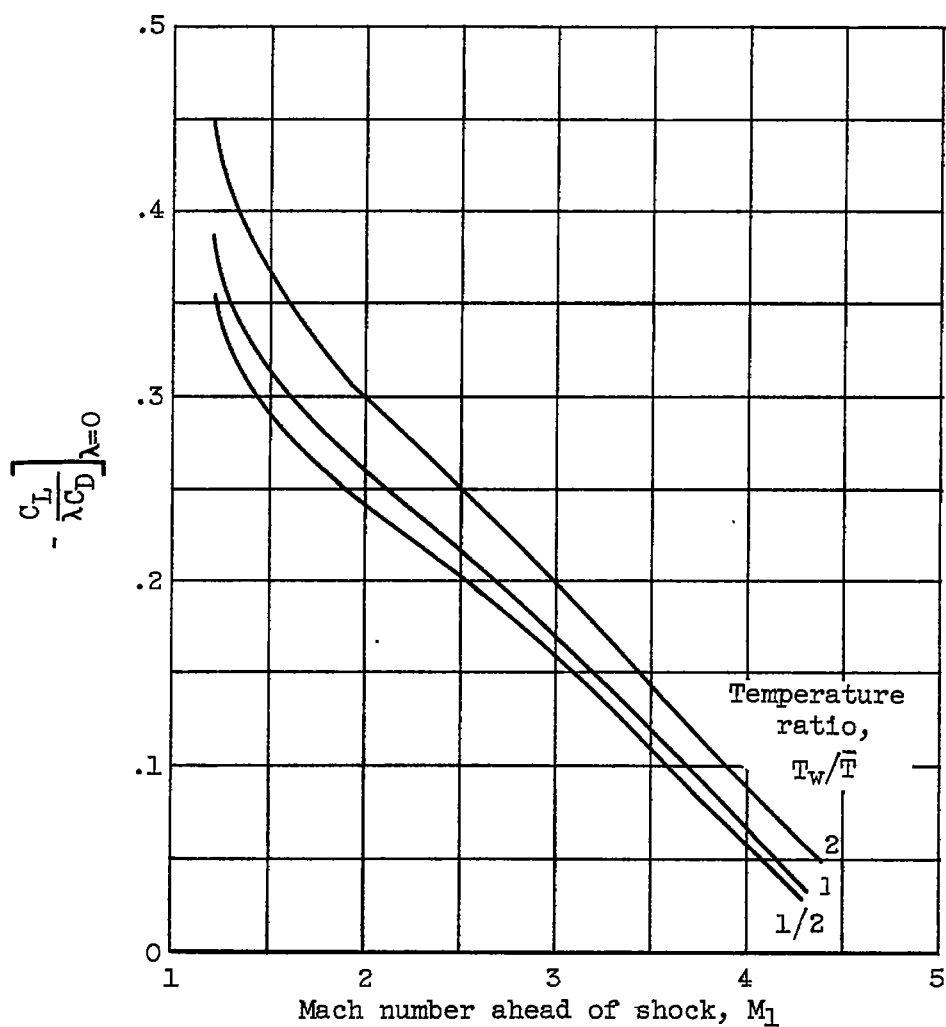
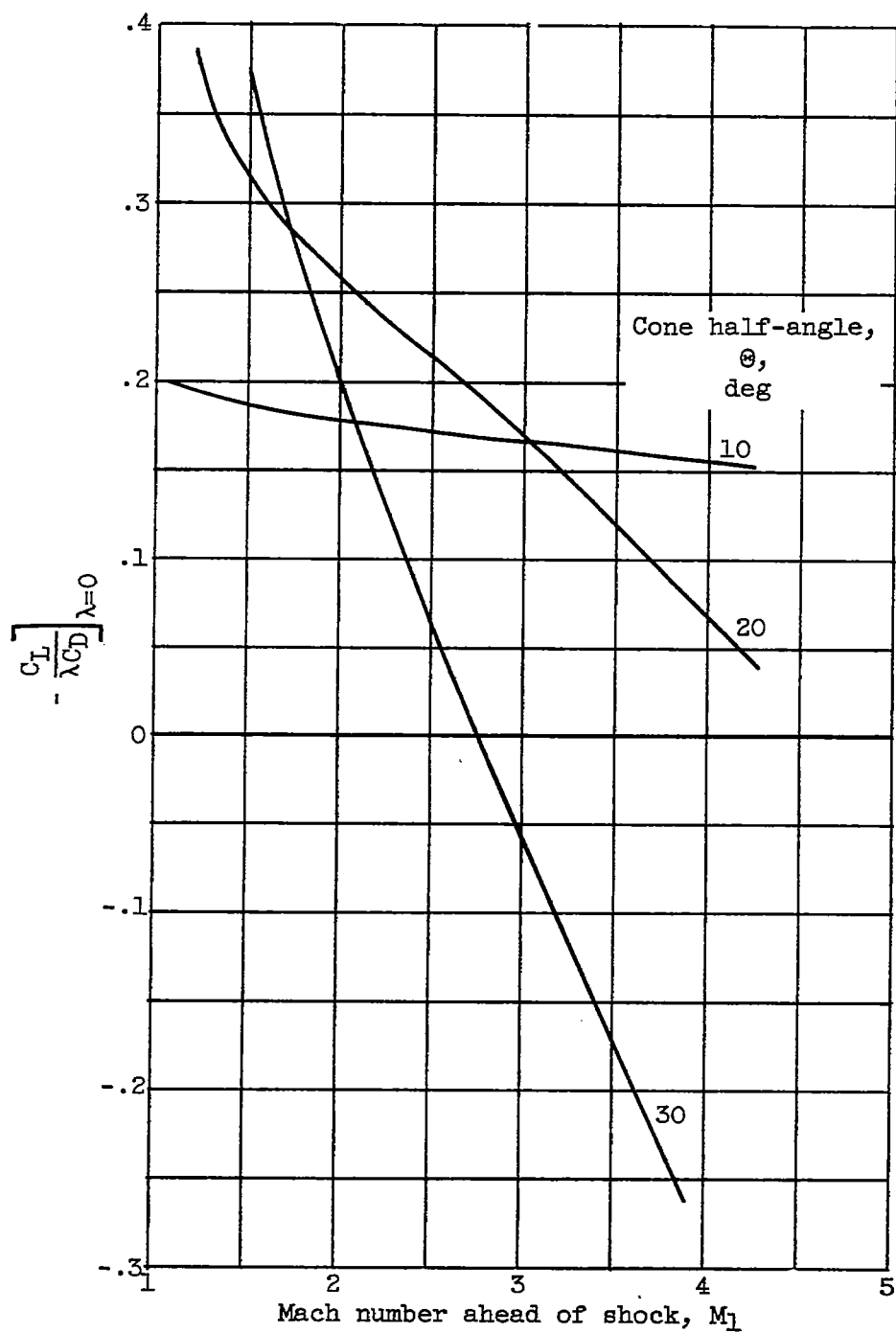
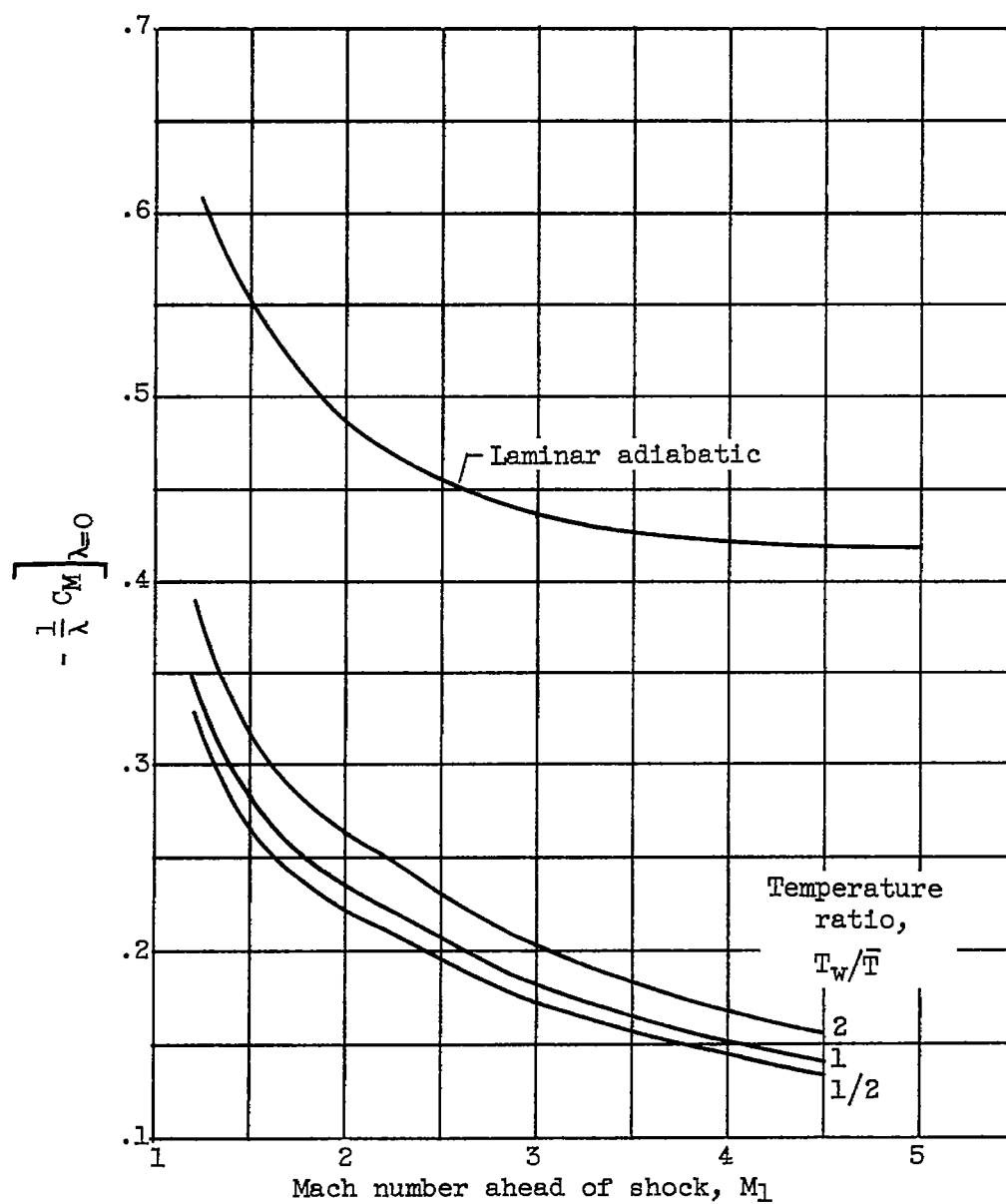
(a) Cone half-angle, 20° .

Figure 6. - Lift on a yawed cone.



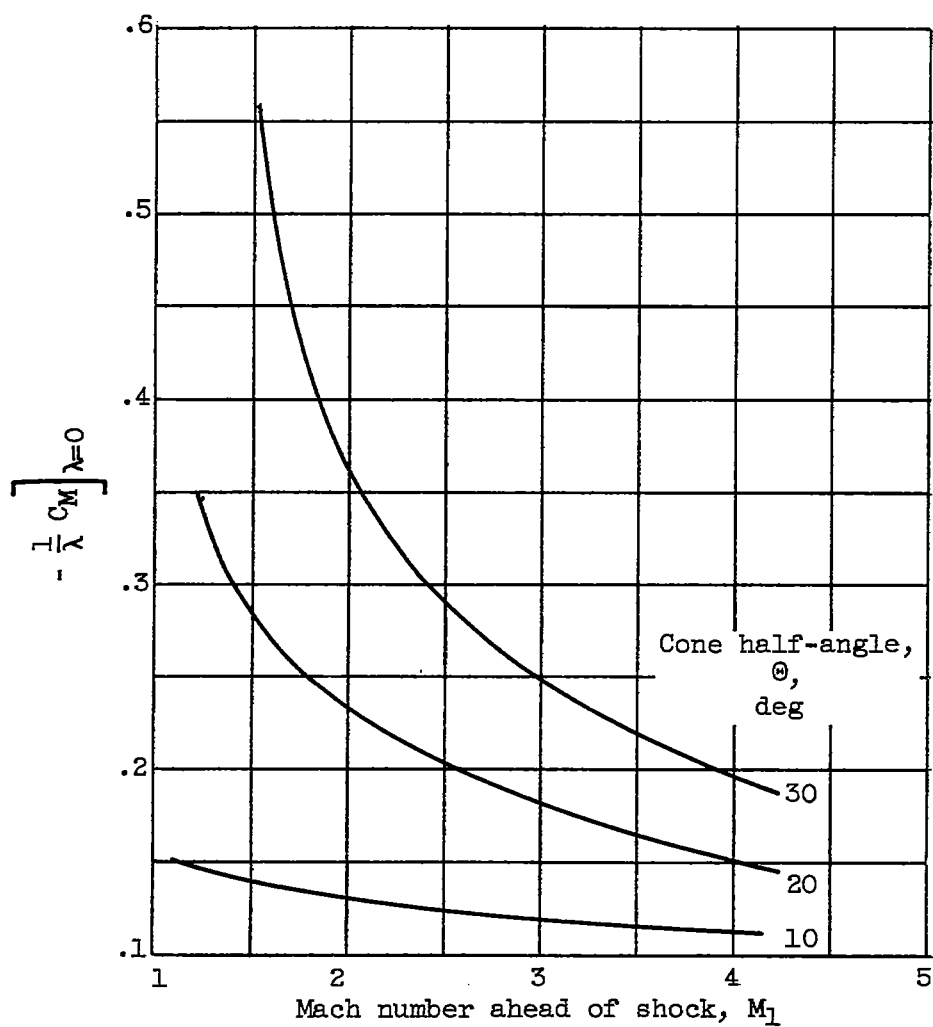
(b) Temperature ratio, T_w/\bar{T} , 1.

Figure 6. - Concluded. Lift on a yawed cone.



(a) Cone half-angle, 20° .

Figure 7. - Pitching moment.



(b) Temperature ratio, T_w/\bar{T} , 1.

Figure 7. - Concluded. Pitching moment.